

the donor wave function may be squeezed already in $d \approx 9$ nm SiNWs estimated from the Bohr radius of the EMT dopants in bulk Si with assuming that the dielectric constant of this SiNW is about the same as that of the bulk. Hence, we can expect to enter the quantum confinement regime for $d \leq 9$ nm and the ionization energy of the EMT donors has to be determined for thinner wires.

This issue has been recently addressed,^{15,17,18} parallel to our study. Diarra and co-workers¹⁵ used an *empirical* tight-binding (TB) method, where the parameters and the perturbing potential of the dopants were fitted from bulk Si data. The interaction between the carrier (electron or hole) and the surface polarization charges induced by its own presence were included by an effective dielectric medium model. While this methodology may work perfectly for large SiNWs, one should question whether accurate values can be obtained in the quantum confinement regime, $1 \text{ nm} \leq d \leq 9$ nm, especially close to the lower limit, where, for instance, local relaxation effects may result in structural configurations that do not appear in bulk Si. On the other hand, the smaller wires can be directly studied by *ab initio* standard density-functional theory (DFT) free of empirical parameters, where the structure and ground-state properties can be determined with great accuracy. However, as is well known, this method *underestimates the band gap* and one cannot rely either on the calculated ionization energies of dopants. This is an especially serious problem in the quantum confinement regime since the fundamental gap is opened and no simple empirical correction can be applied to the DFT ionization energies.

These two methods predicted quite different behavior for $4 \text{ nm} \leq d \leq 20$ nm SiNWs: while according to TB the doping efficiency starts to decrease already at $d \leq 20$ nm, within DFT calculations the ionization energies are still very shallow in $d \geq 3$ nm SiNWs.¹⁸ These results are not conclusive due to the deficiencies of both methodologies concerning this important issue. State-of-the-art time-dependent DFT (TD-DFT) or many-body perturbation theory, like GW,¹⁹ would be the best suited choice to study the dopant states in SiNWs, but they are computationally prohibitive even for very small *defective* wires, e.g., $d \approx 1.0$ nm. Recently,²⁰ we demonstrated that by using a well-chosen *ab initio* hybrid functional within DFT (i) we were able to calculate relatively large SiNWs directly and (ii) the calculated electronic band gaps of the SiNWs with different sizes were in excellent agreement with the experimental results,¹⁶ as well as with GW calculations.²¹ The aim of this paper is applying this methodology to the study of EMT donors in hydrogenated SiNWs.

In this work (i) we show that in accordance with one-dimensional hydrogen theory, the donor dopants show typical EMT states even at $d \approx 1.5$ nm, and their wave function are highly localized in the quantum confinement regime; the EMT state breaks down only at about $d \approx 1.0$ nm; (ii) we provide the hyperfine constant of phosphorus to identify it in SiNWs and we establish the connection between its hyperfine constant and ionization energy; (iii) we show that the ionization energy of dopants are deeper than the values obtained within standard DFT, though the difference decreases for larger wires; (iv) we predict that the doping efficiency for

$d \geq 10$ nm is comparable with that of bulk Si. Although it has been shown that P dopants segregate to the surface, especially in the presence of dangling-bond defects,^{22,23} in our study we consider substitution in the innermost part of the wire. The reason is that we want to focus on the effect of quantum confinement. As we show below, even if the doping into the core is achieved, the donor level is still too deep to act as an efficient dopant.

II. METHODOLOGY

We have performed two sets of DFT calculations. At first we have relaxed the atomic positions until all the forces were lower than $0.02 \text{ eV}/\text{\AA}$ with the SIESTA code,²⁴ using the generalized gradient approximation (GGA) in the Perdew-Burke-Ernzerhof (PBE) parametrization functional²⁵ for the exchange-correlation energy. We have used a 30 \AA vacuum between the wires in the nonperiodic directions and Monkhorst-Pack K -point sampling²⁶ along the wire axis in order to converge the charge density, using an optimized double- ζ polarized basis set and Troullier-Martins pseudopotentials.²⁷ The second set of calculations was carried out with a one-parameter hybrid functional within DFT (Ref. 28) using the optimized GGA geometries. We used the CRYSTAL2003 code,²⁹ using norm-conserving effective core potentials with an optimized $21G^*$ valence basis.³⁰ Besides the PBE functional, 12% Hartree-Fock exchange is mixed into the Hamiltonian. It has been shown that this is the best choice for Si-based materials,³¹ where not only the band gap of bulk Si is reproduced, but also the defect states are obtained with good accuracy.³¹ In CRYSTAL2003 calculations, we used a $6-21G^*$ all-electron basis for the P atom in order to calculate its hyperfine constants in SiNWs. Extending the use of this hybrid-functional Hamiltonian (HFH) to nanostructures could be questioned. However, our HFH has recently proven to perform remarkably well in the calculation of the band gap of hydrogenated SiNWs,²⁰ obtaining good agreement with GW calculations²¹ and experimental results.¹⁶ We also note that a similar HFH was used to successfully study carbon nanotubes³² and graphene nanoribbons.³³

We focus on $\langle 111 \rangle$ and $\langle 110 \rangle$ SiNWs, the wires that are most easily grown and thus are most important for applications. The effective diameters d of these wires were ≈ 1.0 , ≈ 1.5 , and ≈ 2.0 nm. The definition of the diameter of the nanowires is somewhat ambiguous. We defined it as the diameter of the largest circle which can be drawn into the wire excluding the hydrogen atoms,³⁴ using cylindrical shaped SiNWs as indicated by STM measurements.¹⁶ We emphasize that we dealt with *defective* nanowires and that we intended to study *isolated* dopants. The primitive cell of the wires is clearly too small and adding an impurity there would represent an unrealistic doping concentration. Therefore, we used a supercell geometry along the periodic dimension, while allowing the proper vacuum buffer along the transverse dimensions. For small wires the donor wave function is squeezed and its effective Bohr radius is reduced a lot compared to its bulk counterpart, as was discussed above. We used $l \geq 2$ nm for all SiNWs in our study, where l is the supercell lattice constant. This supercell size proved to be

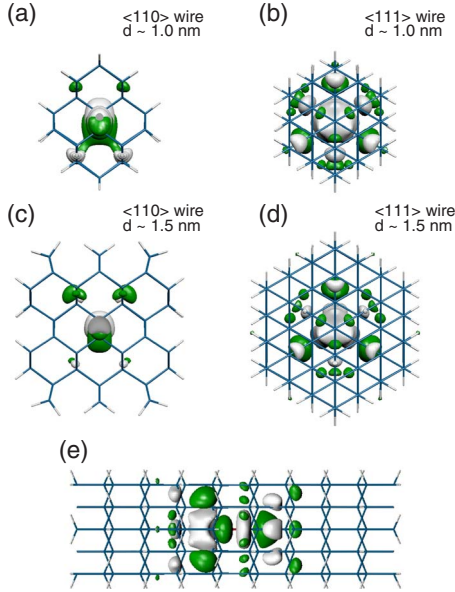


FIG. 1. (Color online) Cross-section view of the donor wave functions in the nanowires studied in the case of P doping [panels (a) to (d)]. For the thinnest $\langle 111 \rangle$ SiNW we also plot a side view [panel (e)] of the nanowire, showing that the chosen computational supercell (here shown in its full length) is large enough to reasonably describe the decay of the P wave function. We plot isosurfaces of the modulus of the wave functions at the Γ point, whereas the dark and light colors correspond to the different phases.

sufficient to allow a proper decay of the impurity wave function [see Fig. 1(e)]. Our largest wire ($\langle 111 \rangle$, $d=2.0$ nm, $l \approx 2.9$ nm) contains 636 atoms, which is close to our computational capacity limit for the HFH CRYSTAL2003 code, and we could not consider directly larger wires. We will show later, however, that we can still estimate the ionization energies of donors in the larger diameter range.

III. RESULTS

A. Ionization energies

We considered P substitutional in the innermost part of the wires in order to calculate their shallowest ionization energies. As we mentioned earlier, surface impurities are expected to provide deeper states for reasons that are beyond quantum confinement. We found that the relaxation of the neighbor atoms next to P is small.

The calculated donor wave function in different wires is shown in Fig. 1 and allows us to conclude several things: (i) the donor wave function is indeed strongly localized compared to their bulk counterpart; (ii) our supercell is acceptably long even for $d=2.0$ nm to describe the *isolated* P donors in our SiNWs. Supercells made of a smaller number of primitive cells would result in an artificial overlap between the donor wave functions that cannot correctly describe the isolated donors; (iii) the donor states in the ultrasmall wires ($d \approx 1.0$ nm) are *qualitatively* different from the larger wires: the donor wave function is well localized within $d \geq 1.5$ nm wires, while it significantly interacts with the surface in $d \approx 1.0$ nm wires: *the donor states cannot be de-*

scribed as quasi-one-dimensional confined EMT states anymore because the surface strongly and directly influence them. On the other hand, it is apparent from Fig. 1 that P donors still exhibit EMT-like donor states in $d \geq 1.5$ nm wires. The large reduction in the Bohr radius of the donor wave function is caused in part by the reduced screening and in part by the two-dimensional quantum confinement effect. Thus, we estimate that the simple quasi-one-dimensional EMT state breaks down at about $d \leq 1.0$ nm. This means that *calculations on shallow dopants carried out in $d \approx 1.0$ nm wires do not provide relevant information that can be extrapolated to larger wires.* Also, even in the relatively small wires $l \geq 2.0$ nm supercells should be used to explore the physics of *isolated* dopants. This is more critical for larger wires because, according to the low-dimensional EMT, the wider the wire the more delocalized donor wave functions are expected to appear. This makes the simulation by *ab initio* methods very challenging since wider wires contain a larger number of atoms in the primitive cell and the corresponding supercell should be larger (made of a larger number of primitive cells) than for smaller wires. We expect that about $l \geq 40$ Å supercell should be used for convergent results for $d \approx 2.5$ nm, amounting to about 1200 atoms. At present, this system is computationally prohibitive for our HFH method. Still, we believe that we could capture the physics of EMT states in $d \approx 1.5$ – 2.0 nm wires that are relevant even for larger wires.

We calculated the ionization energies (E_i) of the P donor. As expected, the DFT-PBE values show too shallow levels because of the self-interaction error. Nevertheless, there is a clear trend indicating that this error shrinks for larger wires. This is not unexpected since standard DFT values for very delocalized states (similar to “metallic” states) works well. However, the error for thin nanowires is not negligible. Due to computational limitations, as discussed above, we cannot calculate larger wires beyond standard DFT. However, we know that if the radius of the wire (R) goes to infinity, then the ionization energy of the P donor will reach $E_i^0 = 0.045$ eV; its dielectric constant will be equal to 11.4, while its effective mass will be about 0.3. We used the function of $E_i^0 + (a/R)^b$ to obtain the ionization energies in the larger wires in the spirit of the TB model developed by Dirra and co-workers¹⁵ (E_i is given in eV, while R and a in nm). This fit function describes both the quantum confinement effect on the donor wave function (reduced Bohr radius of the donor wave function) and the reduced screening.¹⁵ These two effects are dependent on each other and naturally occur in our self-consistent solution. We fit the $a; b$ parameters to the ionization energies of the EMT states ($d = 1.5$ – 2.0 nm) in Table I, obtaining 0.35;1.49 and 0.43;1.56 for $\langle 011 \rangle$ and $\langle 111 \rangle$ wires, respectively. The estimated ionization energies are plotted in Fig. 2.

The decay of the function is very similar to that of the TB results of Ref. 15, but the starting point from the HFH method is much shallower in energy. TB calculations predict ionization energies deeper than 0.7 eV for the P donor in $d = 2.0$ nm wires, whereas the HFH values are about 0.3–0.25 eV, depending on the type of wire. Therefore, in small wires TB *overestimates* the ionization energies, while DFT-PBE *underestimates* them. This has a serious consequence on the

TABLE I. The calculated ionization energies obtained by DFT-PBE and HFH calculation for the given wires in the first column. All values are given in eV with respect to the calculated CBM. In the last column we report the Fermi-contact hyperfine constants $A_{\text{FC}}^{(P)}$ in MHz of the ^{31}P donor in SiNWs given in the first column. As a reference, we give the Fermi-contact term of the ^{31}P donor in bulk Si: 117.5 MHz taken from Ref. 35.

	d	PBE	HFH	$A_{\text{FC}}^{(P)}$
$\langle 011 \rangle$	1.0	0.66	0.93	611.2
	1.5	0.20	0.36	1119.7
	2.0	0.13	0.25	744.6
$\langle 111 \rangle$	1.0	0.31	0.64	1465.2
	1.5	0.23	0.46	1208.4
	2.0	0.19	0.31	794.4

extrapolation of the ionization energies of large wires: while TB predicts a decrease in the doping efficiency already for $d \leq 20$ nm, within standard DFT this happens only for wires as thin as $d \approx 3$ nm. On the other hand, as shown in Fig. 2, within our HFH scheme it is around $d \geq 10$ nm that the ionization energy difference obtained in the wire and in the bulk becomes small (≤ 20 meV) so that the activation of donors is a feasible process at room temperature. According to our calculations the difference vanishes (≤ 1 meV) for $d \geq 71$ nm. This can be explained by the nature of the dielectric screening which decays very slowly as a function of the diameter of the wire. These results qualitatively agree with recent measurements on heavily P-doped SiNWs (Ref. 36) that reported a change in the conductivity already for $d \approx 70$ nm.

B. Hyperfine constant

In silicon quantum dots the isotropic hyperfine constant of P donors could be measured by electron paramagnetic

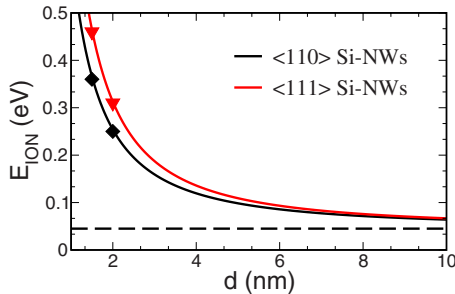


FIG. 2. (Color online) The estimated donor ionization energies for phosphorus dopant in the core of hydrogenated SiNWs as the function of their diameter. The vertical line shows the limit of bulk Si. The calculated data corresponding to ≈ 1.5 and ≈ 2.0 nm SiNWs are shown by diamonds and triangles. The curves are obtained on the basis of a fit that follows the model developed by Diarra *et al.* (Ref. 15) (see text). Notice that the calculated ionization energies of the ≈ 1.0 nm SiNWs have not been used as inputs for the fit (and thus are not displayed) for the reasons explained in the text.

resonance.³⁷ It is useful to calculate the hyperfine constants of the ^{31}P isotope in SiNWs because one can establish a correspondence between the donor wave function and the hyperfine constants as explained below. The hyperfine constants can be calculated as

$$A_{ij}^{(N)} = \frac{1}{2S} \int d^3r n_s(\mathbf{r}) \gamma_N \gamma_e \hbar^2 \left[\left(\frac{8\pi}{3} \delta(r) \right) + \left(\frac{3x_i x_j}{r^5} - \frac{\delta_{ij}}{r^3} \right) \right], \quad (3)$$

where $n_s(\mathbf{r})$ is the spin density of the spin state S , γ_N is the nuclear Bohr magneton of nucleus N , and γ_e is the electron Bohr magneton. The Fermi-contact term, $A_{\text{FC}}^{(N)} = \sum_i A_{ii}^{(N)}/3$, is proportional to the spin density localized at the place of the nucleus which is dominant compared to the dipole-dipole term, $(A_{33} - \sum_i A_{ii}^{(N)})/2$. The ratio of the Fermi-contact and dipole-dipole terms characterizes the shape of the spin density. The contribution of s -like wave functions to the charge density has a large effect on the Fermi-contact term, but a negligible effect on the dipole-dipole term (since the s -like wave function has a maximum at the positions of the nuclei and it is an even function), while the contribution of p -like wave functions to the charge density has a negligible effect on the Fermi-contact term, but a large effect on the dipole-dipole term (since the p -like wave function has a node at the place of nuclei and it is an odd function).

The P donor has a $1s$ ground state possessing A_1 symmetry in bulk Si, which implies that only the Fermi-contact term occurs for ^{31}P , as indeed measured.³⁵ Unless the EMT state does not break down, the EMT donor state in SiNWs shows similar features like in bulk Si so the hyperfine field will be dominated by the Fermi-contact term. The Fermi-contact term is proportional to $|\psi_s^P(0)|^2$, where $\psi_s^P(r)$ is the s -like wave function of a P atom. Finally, the more localized EMT donor implies a larger Fermi-contact term and it can be used as an *indirect measure* of the effect of quantum confinement.^{37,38}

We have calculated the hyperfine constants of P impurities in the SiNWs considered. The results are summarized in Table I. One can see that the Fermi-contact term in all cases shows much larger values than in bulk Si. Besides that, the values decrease with the increasing size of the SiNWs, except $\langle 011 \rangle$ wires. However, we already showed above that the EMT state breaks down in the $d \approx 1.0$ nm wire, especially in the small $\langle 011 \rangle$ wire, and the wave function shows different character compared to others. This also reflects in its hyperfine constants. The dipole-dipole term of that donor is 17.4 MHz that implies a sizeable dangling-bond-like hybridization with the neighbor atoms. For the $\langle 111 \rangle$ wire with $d=1.0$ nm this value is much smaller, though measurable, 4.07 MHz. In the $\langle 011 \rangle$ wire we observed that the donor wave function is very squeezed in the nonperiodic directions, forcing the wave function to spread along the periodic direction of the wire. This delocalization is completely different from the usual EMT donor states in larger wires, showing the spherical shape of the donor wave function.

For the $d \geq 1.5$ nm wires, the envelope function of the donor ground state can be described as $\Psi(r) = \sqrt{\pi/a_B^3} \exp(-r/a_B)$, provided that the P atom resides in the inner part of

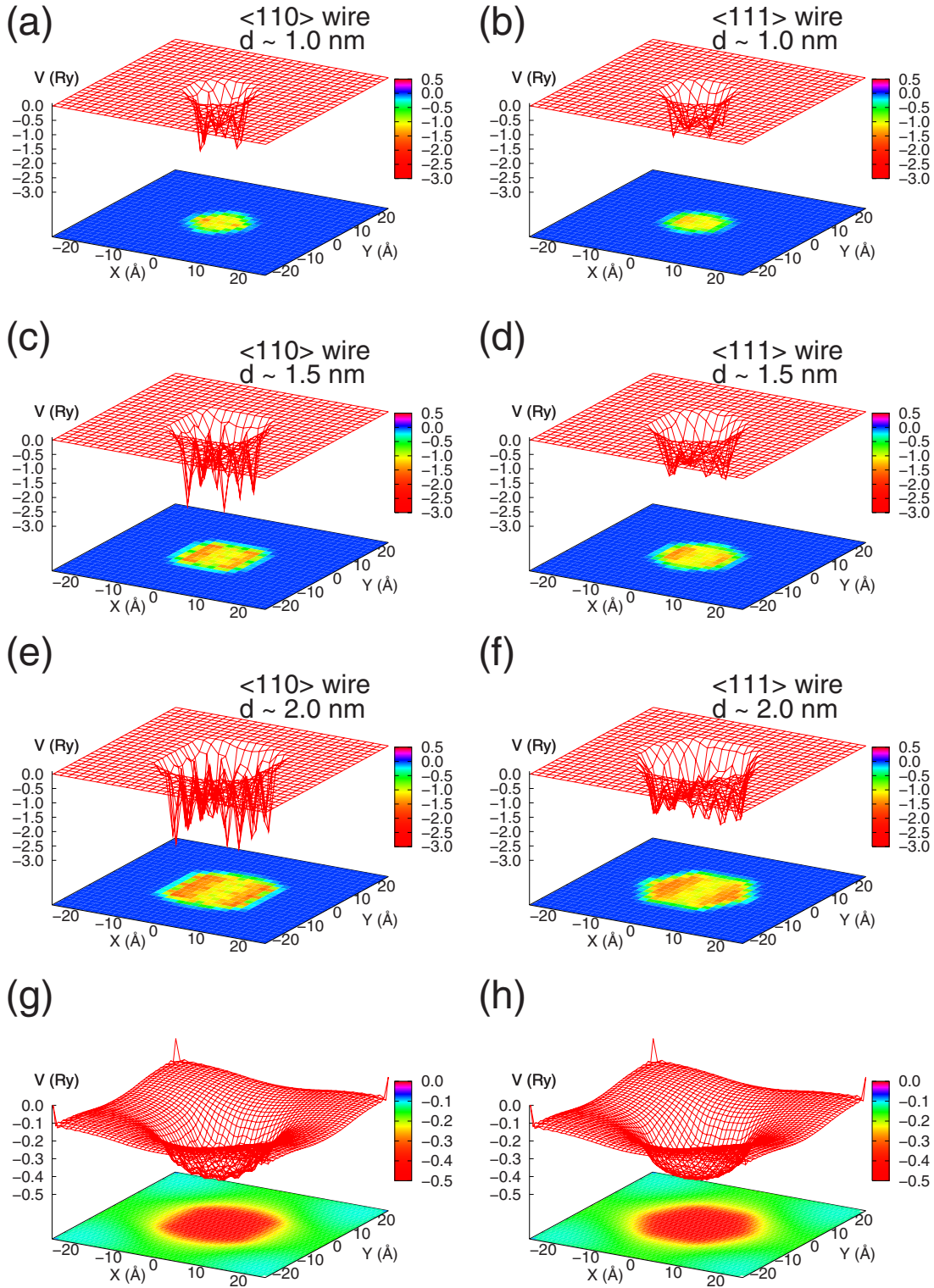


FIG. 3. (Color online) The calculated total potential surface averaged in the periodic axis for the different wires [panels (a) to (f)]. This shows the two-dimensional confinement potential for the quasi-free donor electron. In panels (g) and (h) the average potential surface of panels (e) and (f) has been smoothed in order to hide the details coming from the atomistic details.

the wire. Considering this EMT donor state one can establish that the donor wave function is expected to be about $10\times$ more localized in $d \approx 1.5$ nm wires than in bulk Si. This is consistent with the drawn wave function shown in Fig. 1. In $d \approx 2.0$ nm wires this number reduces already to about 6

$\approx 744/117$. Indeed, large supercells are needed even for $d \approx 2.5$ nm wires to describe the isolated EMT donors.

The hyperfine constants can be used as an indirect probe into whether the P donor indeed substitutes a core Si atom or is placed at the surface. The closer the P donor to the surface

the more the wave function deviates from the spherical shape. This means that the dipole-dipole hyperfine interaction will appear for those P donors which are close to the surface.

By assuming that the effective mass does not change significantly in the wires compared to its bulk value,³⁹ one can find the following connection between the Fermi-contact hyperfine constant of the P donor and its ionization energy:

$$A_{\text{FC}}^{(P)}(R) \sim [E_i(R)]^3 \epsilon^3(R), \quad (4)$$

where $E_i(R)$ is the ionization energy of the P donors in the wire with the radius of R . Using this formula we predict that the dielectric constants in the ultrathin wires decrease to about one third of the dielectric constant of bulk Si. A similar feature is expected in silicon nanocrystals.³⁸ Although capturing the right trend of the dielectric constant, this model might be oversimplified since we do not take into account the space dependence of the dielectric constant. First-principles calculations of the static dielectric properties of nanowires⁴⁰ provide higher average values for ϵ , where they calculated the space-dependent dielectric constant.

IV. DISCUSSION

We have discussed the results for the *shallowest* donor in silicon confined into the wire. Naively, we expect that the deeper donor levels than that of the P donor in bulk Si will result in also deeper donor levels in the wires. However, Durgun and co-workers¹⁷ showed shallower levels for arsenic than for phosphorus in thin SiNWs. We note that the calculation were made in a very small supercell that may not be realistic. Nevertheless, local relaxation effects may change the order of levels of different dopants in the quantum confinement regime. Therefore, we also investigated arsenic in $\langle 110 \rangle$ and $\langle 111 \rangle$ SiNWs of 1.0 and 1.5 nm diameter. For these dopants, as our purpose was simply outlining a trend, we restricted ourselves to DFT-PBE calculations. We found that As basically behaves like P, although it has somewhat *deeper* ionization energies (by about 0.03 eV) than the P donor in wires of the same diameter. Arsenic is not an ideal dopant for biological applications; therefore, we also studied the doping efficiency of sulfur. Sulfur is a double donor in bulk Si; its first ionization energy is about 0.3 eV. This state can be described by the same effective-mass theory like for

column V dopants, but the electron-electron interaction on the $1s$ ground state will lower its ionization energy. We found that this characteristic behavior persists also in SiNWs. We have found that the EMT state breaks down in $d=1.0$ nm wires while it works for $d=1.5$ nm wires; therefore, we conclude that the *EMT theory squeezed into quasi-one-dimension can be generalized for every EMT dopant (including the acceptors) in SiNWs*. In Fig. 3 we plot the calculated total potential that the quasi-free donor electron feel in the wires.

In order to have a qualitative picture we averaged the potential along the periodic axis. The resulted potential surface shows clearly the quantum confinement of the electron in two dimensions. Apart from the atomistic details, the potential surface shows almost the same depth for all the wires *independently on its orientation and size*, while naturally the width of the potential well increases with the increasing diameter of the wires. Actually, the potential surface shows a paraboloidlike shape, but it is difficult to achieve even a semiquantitative analysis. Nevertheless, simple quantum-mechanical calculation arguments are consistent with the results of the self-consistent calculations: the ionization energies decrease with increasing size of the wires.

V. SUMMARY

In summary, we studied the EMT donors in silicon nanowires. We found that *generally* the EMT levels will be much deeper in ultrathin silicon nanowires than in bulk silicon, but we predict that the doping efficiency will be almost perfect for wires that have larger diameter than 10 nm. In addition, we provide hyperfine constants for the shallowest donor, phosphorus, in thin nanowires and we show that there is a simple connection with the ionization energies. We suggest that measurements of the hyperfine constants can be used as a probe for the detection of the location of the impurities in the wires.

ACKNOWLEDGMENTS

A.G. acknowledges support from OTKA under Contract No. K-67886. R.R. is supported by the Ramón y Cajal program of Ministerio de Ciencia e Innovación and acknowledges funding under Contract No. TEC2006-13731-C02-01.

¹Y. Li, F. Qian, J. Xiang, and C. M. Lieber, *Mater. Today* **9**, 18 (2006).

²Y. Cui and C. M. Lieber, *Science* **291**, 851 (2001).

³G. Zheng, W. Lu, S. Jin, and C. M. Lieber, *Adv. Mater.* **16**, 1890 (2004).

⁴J. Xiang, W. Lu, Y. Hu, H. Yan, and C. M. Lieber, *Nature (London)* **441**, 489 (2006).

⁵P. Zhang, E. Tevaarwerk, B. Park, D. Savage, G. Celler, I. Knezevic, P. Evans, M. Eriksson, and M. Lagally, *Nature (London)* **439**, 703 (2006).

⁶R. Rurali and N. Lorente, *Phys. Rev. Lett.* **94**, 026805 (2005).

⁷R. Rurali, A. Poissier, and N. Lorente, *Phys. Rev. B* **74**, 165324 (2006).

⁸Y. Cui, Z. Zhong, D. Wang, W. Wang, and C. Lieber, *Nano Lett.* **3**, 149 (2003).

⁹F. Patolsky and C. M. Lieber, *Mater. Today* **8**, 20 (2005).

¹⁰F. Patolsky, G. Zheng, and C. M. Lieber, *Anal. Chem.* **78**, 4260 (2006).

¹¹Y. Cui, Q. Wei, H. Park, and C. M. Lieber, *Science* **293**, 1289 (2001).

- ¹²B. Tian, X. Zheng, T. J. Kempa, Y. Fang, N. Yu, G. Yu, J. Huang, and C. M. Lieber, *Nature (London)* **449**, 885 (2007).
- ¹³T. J. Kempa, B. Tian, D. R. Kim, J. Hu, X. Zheng, and C. M. Lieber, *Nano Lett.* **8**, 3456 (2008).
- ¹⁴R. Loudon, *Am. J. Phys.* **27**, 649 (1959).
- ¹⁵M. Diarra, Y.-M. Niquet, C. Delerue, and G. Allan, *Phys. Rev. B* **75**, 045301 (2007).
- ¹⁶D. D. D. Ma, C. S. Lee, F. C. K. Au, S. Y. Tong, and S. T. Lee, *Science* **299**, 1874 (2003).
- ¹⁷E. Durgun, N. Akman, C. Ataca, and S. Ciraci, *Phys. Rev. B* **76**, 245323 (2007).
- ¹⁸C. R. Leao, A. Fazzio, and A. J. R. da Silva, *Nano Lett.* **8**, 1866 (2008).
- ¹⁹F. Aryasetiawan and O. Gunnarsson, *Rep. Prog. Phys.* **61**, 237 (1998).
- ²⁰R. Rurali, B. Aradi, T. Frauenheim, and A. Gali, *Phys. Rev. B* **76**, 113303 (2007).
- ²¹M. Bruno, M. Palummo, A. Marini, R. Del Sole, and S. Ossicini, *Phys. Rev. Lett.* **98**, 036807 (2007).
- ²²M. V. Fernández-Serra, Ch. Adessi, and X. Blase, *Phys. Rev. Lett.* **96**, 166805 (2006).
- ²³H. Peelaers, B. Partoens, and F. Peeters, *Nano Lett.* **6**, 2781 (2006).
- ²⁴D. Sánchez-Portal, P. Ordejón, E. Artacho, and J. M. Soler, *Int. J. Quantum Chem.* **65**, 453 (1997).
- ²⁵J. P. Perdew, K. Burke, and M. Ernzerhof, *Phys. Rev. Lett.* **77**, 3865 (1996).
- ²⁶H. J. Monkhorst and J. K. Pack, *Phys. Rev. B* **13**, 5188 (1976).
- ²⁷N. Troullier and J. L. Martins, *Phys. Rev. B* **43**, 1993 (1991).
- ²⁸A. D. Becke, *J. Chem. Phys.* **104**, 1040 (1996) and references therein.
- ²⁹V. R. Saunders *et al.*, *CRYSTAL2003 User's Manual* (University of Torino, Torino, 2003).
- ³⁰M. Causà, R. Dovesi, and C. Roetti, *Phys. Rev. B* **43**, 11937 (1991).
- ³¹P. Deák, A. Gali, A. Sólyom, A. Buruzs, and T. Frauenheim, *J. Phys.: Condens. Matter* **17**, S2141 (2005).
- ³²V. Barone, J. Peralta, M. Wert, J. Heyd, and G. Scuseria, *Nano Lett.* **5**, 1621 (2005).
- ³³V. Barone, O. Hod, and G. Scuseria, *Nano Lett.* **6**, 2748 (2006).
- ³⁴T. Vo, A. J. Williamson, and G. Galli, *Phys. Rev. B* **74**, 045116 (2006).
- ³⁵G. Feher, *Phys. Rev.* **114**, 1219 (1959).
- ³⁶M. T. Bjork, H. Schmid, J. Knoch, H. Riel, and W. Riess, *Nat. Nanotechnol.* **4**, 103 (2009).
- ³⁷M. Fujii, A. Mimura, S. Hayashi, Y. Yamamoto, and K. Murakami, *Phys. Rev. Lett.* **89**, 206805 (2002).
- ³⁸T.-L. Chan, M. Tiago, E. Kaxiras, and J. Chelikowsky, *Nano Lett.* **8**, 596 (2008).
- ³⁹J.-A. Yan, L. Yang, and M. Y. Chou, *Phys. Rev. B* **76**, 115319 (2007).
- ⁴⁰S. Hamel, A. J. Williamson, H. F. Wilson, F. Gygi, G. Galli, E. Ratner, and D. Wack, *Appl. Phys. Lett.* **92**, 043115 (2008).